# Turnip mosaic virus is a second example of a virus using transmission activation for plant-to-plant propagation by aphids

Edwige Berthelot, Marie Ducousso, Jean Luc Macia, Florent Bogaert, Volker Baecker, Gael Thébaud, Romain Gallet, Michel Yvon, Stéphane Blanc, Mounia Khelifa, et al.

JVI Accepted Manuscript Posted Online 13 February 2019
J. Virol. doi:10.1128/JVI.01822-18




# Turnip mosaic virus is a second example of a virus using transmission activation for plant-to-plant propagation by aphids

Edwige Berthelot [a,b,c], Marie Ducousso [a], Jean-Luc Macia [a], Florent Bogaert [d], Volker Baecker [e], Gaël Thébaud [a], Romain Gallet [a], Michel Yvon [a], Stéphane Blanc [a], Mounia Khelifa [b,c,#]¶, Martin Drucker [a,d,#]

[a] BGPI, INRA Centre Occitanie, SupAgro, CIRAD, Université de Montpellier, Montpellier, France

[b] Semences Innovation Protection Recherche et Environnement, Achicourt, France

[c] Fédération Nationale des Producteurs de Plants de Pomme de Terre, Paris, France

[d] SVQV, INRA Centre Grand Est, Université de Strasbourg, Colmar,

[e] France Montpellier Ressources Imagerie, Biocampus Montpellier, CNRS, INSERM, Université de Montpellier, Montpellier, France[#]

Corresponding authors. E-mail mounia.khelifa@u-picardie.fr and martin.drucker@inra.fr

## Abstract

Cauliflower mosaic virus (CaMV, family *Caulimoviridae*) responds to the presence of aphid vectors on infected plants by forming specific transmission morphs. This phenomenon, coined transmission activation (TA), controls plant-to-plant propagation of CaMV. A fundamental question is whether other viruses rely on TA. Here, we demonstrate that transmission of the unrelated Turnip mosaic virus (TuMV, family *Potyviridae*) is activated by the reactive oxygen species $H_2O_2$ and inhibited by the calcium channel blocker $LaCl_3$. $H_2O_2$-triggered TA manifested itself by the induction of intermolecular cysteine bonds between viral HC-Pro molecules and by formation of viral transmission complexes, composed of TuMV particles and HC-Pro that mediates vector-binding. Consistently, $LaCl_3$ inhibited intermolecular HC-Pro cysteine bonds and HC-Pro interaction with viral particles. These results show that TuMV is a second virus using TA for transmission, but using an entirely different mechanism than CaMV. We propose that TuMV TA requires ROS and calcium signaling and that it is operated by a redox switch.


## Importance

Transmission activation, i.e. a viral response to the presence of vectors on infected hosts that regulates virus acquisition and thus transmission, is an only recently described phenomenon. It implies that viruses contribute actively to their transmission, something that has been shown before for many other pathogens but not for viruses. However, transmission activation has been described so far for only one virus, and it was unknown whether other viruses rely also on transmission activation. Here we present evidence that a second virus uses transmission activation, suggesting that it is a general transmission strategy.


## Key words

Plant virus; aphid vector; host plant; virus transmission; virus vector host interactions; reactive oxygen species; calcium; signaling


## Abbreviations

CaMV, cauliflower mosaic virus; TuMV, turnip mosaic virus; TA, transmission activation; ROS, reactive oxygen species; TB, transmission body; HC, helper component; HC-Pro, helper component protease; CP, capsid protein

## Introduction

Transmission is an obligatory step in the life cycle of parasites but it is also an Achilles's heel, because parasites must leave the comparably comfortable environment of the host they are installed in, and face a potentially adverse environment during the passage to a new host. Some pathogens rely on resistant dormant states like spores to persist in the "wild" until they reach a new host passively, e.g. carried by the wind. Most pathogens, however, actively use vectors for transmission and they can manipulate both hosts and vectors in an impressive number of ways, all potentially increasing transmission (1–4). In the most sophisticated cases, pathogens "*use exquisitely controlled mechanisms of environmental sensing and developmental regulation to ensure their transmission*" (5). This concept, implying active contribution of the pathogen, is widely accepted for eukaryotic parasites (for example plasmodium, shistosoma, wucheraria, dicrocoelium), which developed fascinating transmission cycles to control and adapt vector-host or primary-secondary host interactions for their propagation (4). We have recently discovered a remarkable phenomenon for a virus. Cauliflower mosaic virus (CaMV, family *Caulimoviridae*) responds to the presence of aphid vectors on infected host plants by forming transmission morphs at the exact time and location of the plant-aphid contact (6). This process, coined Transmission Activation or TA (7), is characterized by the formation of transmission complexes between CaMV virus particles and the transmission helper component (HC), the CaMV protein P2, which mediates vector-binding (1). P2 and virus particles are spatially separated in infected cells since the cell's pool of P2 is retained in specific cytoplasmic inclusions called transmission bodies (TBs) while most virus particles are contained in another type of viral inclusion, the virus factories (8, 9). In such cells, aphid punctures trigger instant disruption of TBs and the liberated P2 relocalizes onto microtubules. Simultaneously, the virus factories release virus particles that associate with P2 on the microtubules (10) to form P2/virus particle complexes, which is the virus form that aphid vectors can acquire and transmit. TA is transient; P2 reforms a new TB (6) and the virus particles return to virus factories (10) after aphid departure. TA implies that CaMV passes, induced by yet unknown mechanisms, from a non-transmissible to a transmissible state. It has been suggested that this phenomenon exists to economize host resources and to invest energy in transmission only when relevant, i.e. in the presence of vectors (7). Whether this hypothesis is true or not, inhibiting TA inhibits transmission, pointing to the importance of TA for CaMV. A fundamental question that arises is whether TA, which is reminiscent of the active transmission strategies employed by eukaryotic parasites, is exclusive to CaMV or whether it could be a general phenomenon in the virus world. Therefore, we studied transmission of the turnip mosaic virus (TuMV, family *Potyviridae*), which is entirely unrelated to CaMV, but uses also an HC for aphid transmission. The HC of TuMV and of other potyviruses is the viral protein helper component protease (HC-Pro). It is a multifunctional protein that other its HC function bears no structural, functional or other similarity with P2. Our results show that TuMV is a second virus relying on TA for transmission, but using a totally different mechanism.

## Results and discussion

### *Signaling molecules modify TuMV transmission by aphids*

TA requires a signaling cascade that connects the initial recognition of the presence of aphids, most likely via a yet unknown elicitor, with a cellular response that is hijacked by the virus. Since TA is fast for CaMV and likely also for TuMV, which uses the same transmission mode, reactive oxygen species (ROS) or calcium are good signaling candidates. We therefore tested the effect of the ROS signaling compound hydrogen peroxide ($H_2O_2$), and of a general inhibitor of calcium signaling, lanthanum(III)chloride ($LaCl_3$), on TuMV transmission, using infected protoplasts as virus source (6, 11). Aphid transmission tests performed with $H_2O_2$-treated protoplasts showed a drastic increase of TuMV transmission (Figure 1A) whereas treatment of protoplasts with $LaCl_3$ caused a strong reduction of transmission (Figure 1B). This effect was not due to modified cell viability (Figure 1C,D). Furthermore, transmission increase by $H_2O_2$ and inhibition by $LaCl_3$ was clearly a biological effect requiring living cells, since no effect was observed when the experiments were repeated using cell extracts, i.e. dead cells (Figure 1E,F). The same control experiments indicate also that $H_2O_2$ and $LaCl_3$ did not modify aphid feeding behavior, which might have been an alternative explanation for the observed differences in transmission rates. Taken together, our data show that TuMV transmission can be artificially enhanced or inhibited.

The protoplast system is a useful but simplified biological system because the cells are individualized and not in their natural symplasmic context in a tissue. Hence, we sought to validate the protoplast results by using leaves on intact infected plants as virus source. We applied $H_2O_2$ or $LaCl_3$ to leaves by spraying treatment (12) and used these plants for aphid transmission assays. To rule out any interference, only one leaf of the same developmental stage was sprayed on each plant and different plants were used for each condition. $H_2O_2$ treatment increased significantly and $LaCl_3$ treatment decreased significantly plant-to-plant transmission rates of TuMV (Figure 1G,H). This confirmed the results obtained with protoplasts and showed that TuMV TA is observed similarly in intact plants. Compared to the protoplast experiments, higher $H_2O_2$and $LaCl_3$ concentrations were required to observe significant effects. This was probably due to dilution of these substances during leaf penetration. Combined, these results suggest that the TA phenomenon exists for TuMV, like for CaMV, and that calcium and ROS signaling might be important for TA of TuMV.

*The increase in virus transmission correlates with the formation of HC-Pro/TuMV transmissible complexes*

Next, we wanted to know how TuMV TA manifests itself in infected cells. TA of CaMV is characterized by relocalization of CaMV particles and CaMV helper protein P2 from viral inclusions to microtubules (6, 10). Therefore, we performed immunofluorescence experiments on TuMV-infected protoplasts with antibodies directed against HC-Pro and the viral capsid protein CP to determine whether $H_2O_2$ and $LaCl_3$ induced relocalization of TuMV virus particles and/or HC-Pro. In untreated cells, HC-Pro and CP localized in the cytoplasm as reported for other potyviruses (13, 14). Treatment with $H_2O_2$ and $LaCl_3$ did not induce any visible rearrangement of HC-Pro or of CP (Figure 2). Thus, TA of TuMV is not characterized by the redistribution of HC-Pro and/or virus particles within infected cells.

We thus hypothesized that HC-Pro and virus particles, both evenly distributed in the cytoplasm, could pass from a non-associated state to an associated state, i.e. to transmissible HC-Pro-virion complexes, upon TA. To visualize such complexes *in situ*, we resorted to the Duolink® technique (15), an antibody-based version of the proximity ligation assay allowing detection of intermolecular interactions. Duolink® performed with HC-Pro and CP antibodies showed that $H_2O_2$ treatment indeed increased the number and intensity of HC-Pro/CP interaction spots (Figure 3A,B), indicative of binding of HC-Pro to virus particles. Interestingly, incubation of protoplasts with $LaCl_3$ decreased the number of transmissible complexes (Figure 3C). Thus, the increase and decrease of HC-Pro/CP interactions, triggered by application of ROS or of a calcium channel blocker, respectively, correlated with an increase and decrease of transmission (compare Figures 1 and 3).

*Transmission activation of TuMV is characterized by formation of cysteine bridges between HC-Pro molecules*

We wanted to understand how HC-Pro and virus particles could rapidly transit from "free" to virus-associated forms. Since ROS like $H_2O_2$ change directly or indirectly the cellular redox potential, the formation of HC-Pro/TuMV transmissible complexes might be controlled by the redox state of HC-Pro and CP, both of which contain cysteine residues that can form disulfide bridges under oxidizing conditions. Therefore, we performed non-reducing SDS-PAGE/Western blots to detect HC-Pro and CP migration profiles altered by intramolecular or intermolecular cysteine disulfide bridges. $H_2O_2$ and $LaCl_3$ did not modify the migration profile of CP (Figure 4A). However, $H_2O_2$ treatment increased the amount of oligomeric HC-Pro and especially of its dimeric form (Figure 4B) that was previously reported to be active in transmission (16–18). $LaCl_3$ treatment had the inverse effect and decreased the amount of HC-Pro oligomers (Figure 4B). The effect of $H_2O_2$ was concentration-dependent and clearly visible using physiologic $H_2O_2$ concentrations (0.25 mM, Figure 4C). Thus, the increase in transmission induced by $H_2O_2$ correlated not solely with formation of HC-Pro/TuMV complexes, but also with the appearance of HC-Pro oligomers hold together by intermolecular cysteine bridges.

To have a biological significance, HC-Pro oligomerization should be completed within the duration of an aphid puncture, i.e. within seconds. Kinetics of formation and breakup of HC-Pro oligomers showed that both occurred within 5 seconds of incubation with $H_2O_2$ and $LaCl_3$, respectively (Figure 4D,E). The effect of both treatments was transient because HC-Pro oligomers disappeared ($H_2O_2$) or reappeared ($LaCl_3$) after ~30 min incubation. Furthermore, removal of $H_2O_2$ by washing protoplasts showed reversibility of HC-Pro oligomerization (Figure 4D). Induction of HC-Pro oligomers by $H_2O_2$ was not restricted to TuMV or to turnip hosts, because experiments with lettuce protoplasts infected with another potyvirus, *Lettuce mosaic virus*, yielded similar results (not shown).

To better establish that formation of disulfide bridges between HC-Pro monomers contributes to oligomerization, infected protoplasts were treated with the disulfide bonds-reducing agent dithiotreitol (DTT) or with N-ethylmaleimide (NEM) that does not break existing disulfide bridges but prevents formation of new ones by blocking free thiols. Figure 4F shows that DTT treatment abolished appearance of $H_2O_2$-induced HC-Pro oligomers in SDS-PAGE/Western blot. This confirmed that oligomerization of HC-Pro requires establishment of intermolecular disulfide bridges. NEM treatment blocked the appearance of HC-Pro oligomers in SDS-PAGE/Western blots when applied before the $H_2O_2$ treatment, but NEM did not prevent their appearance when applied after $H_2O_2$ treatment (Figure 4G). This is a further confirmation of the involvement of disulfide bridges in HC-Pro oligomerization. Note that NEM treatment caused a mobility shift of HC-Pro. This might have been due to disulfide shuffling during denaturation of the samples as reported for papilloma virus (19). To establish a direct role of intermolecular HC-Pro disulfide bonds in TuMV transmission, we performed transmission assays. Because of the toxicity of NEM, we did not use plants as virus source but resorted to the protoplast system where exposure of aphids (and the experimenter) to the substance is minimized by confining it in the protoplast medium. The NEM treatment reduced virus transmission drastically (Figure 4H) but did not affect protoplast viability (Figure 4I), suggesting that *de novo* formation of intermolecular HC-Pro disulfide bonds is required for formation of transmissible complexes and thus for aphid acquisition of TuMV.

*Model of TuMV transmission activation*

In this study, we demonstrate that TA exists for a second virus, TuMV. TuMV TA was induced by the ROS $H_2O_2$ and inhibited by the calcium channel blocker $LaCl_3$. ROS and calcium signaling are both important in early perception of parasites including insects (20) and recently aphid punctures were described to induce rapid calcium elevations around feeding sites (21). Since ROS and calcium signaling are often interconnected (22, 23), TuMV TA likely hijacks an early step of at least one of these pathways. The initial eliciting event remains unknown. It might be a direct effect of aphid saliva-contained ROS or ROS-producing peroxidases (24) that are injected into cells during feeding activity. Alternatively, an aphid or aphid-induced plant factor might interact in a classic pathogen-associated molecular pattern (PAMP)-triggered immunity reaction with a pattern recognition receptor (PRR) (25) that prompts calcium and ROS mediated downstream events. Interestingly, a recent study has demonstrated that the red clover necrotic mosaic virus (RCNMV) requires ROS for replication (26). The authors proposed that plant viruses may have evolved a complex mechanism to manipulate the ROS-generating machinery of plants to improve their infectivity, or, transferred to this case, transmission.

TA of TuMV manifests itself by creation of HC-Pro intermolecular disulfide bridges, driven by oxidation of the cellular redox potential. We propose that oxidation of HC-Pro induces a functional switch rendering HC-Pro able to interact with virus particles and form transmissible complexes (Figure 5). Functional switching (moonlighting) by redox-driven modification of disulfide bridges has been reported for other proteins and is operated by conformation changes affecting the secondary, tertiary or quaternary structure of proteins (27–29). Why would there be such a switch? HC-Pro is a multifunctional protein involved not only in aphid transmission (30) but also in pathogenicity (31), viral movement (32) and suppression of plant RNA silencing (33–35). One (or more) functional switches could assist to coordinate these multiple functions by allowing interaction with virions and formation of transmissible complexes only when transmission is possible, i.e. when the aphids puncture cells This would help to economize finite plant resources as proposed earlier (7).

Unfortunately, we cannot provide an empirical proof that the aphid punctures directly trigger TuMV TA. In contrast to CaMV, where TA was directly visible using qualitative immunofluorescence observation of P2 and virus particle networks (the characteristic manifestation of CaMV TA) in cells in contact with aphid saliva sheaths, TuMV TA cannot be revealed by a qualitative analysis. The quantitative Duolink® approach we used to demonstrate TuMV HC-Pro/CP interactions in protoplasts required an enormous number of cells for analysis and statistical validation. Identifying a comparable number of cells in tissue and in contact with aphid stylets is barely feasible. The same restrictions apply to electron microscopy techniques to localize HC-Pro on virus particles by immunogold labeling. Thus, proof of aphid implication in TA of TuMV remains indirect, for the time being.

Nonetheless, we here demonstrate TA for a second virus, TuMV, different from CaMV, suggesting that transmission activation might be a more general phenomenon. The great phylogenetic distance between TuMV and CaMV makes it likely that the phenomenon of TA arose independently for the two viruses during evolution. An obvious question is whether yet other viruses use TA for their transmission.

## Materials and methods

### *Plants, viruses and inoculation*

Turnip plants (*Brassica rapa* cv. Just Right) and lettuce (*Lactuca sativa* cv. Mantilla and Trocadero) were grown in a greenhouse at 24/15 °C day/night with a 14/10 h day/night photoperiod. Two-weeks-old turnip plants were mechanically inoculated with wild-type TuMV strain C42J (36), and two-weeks-old lettuce plants with *Lettuce mosaic virus* (LMV) strain E (37). Plants were used for experiments at 14 days post inoculation (dpi).

### *Isolation of protoplasts*

Protoplasts from turnip leaves were obtained by enzymatic digestion as described (6).

### *Preparation of infected cell extracts*

TuMV-infected turnip protoplasts were sedimented and resuspended in SAKO buffer (500 mM $KPO_4$ and 10 mM $MgCl_2$ pH 8.5) (38). Then sucrose was added to a final concentration of 15 % and the suspension was vortexed to homogenize protoplasts.

### *Drug treatments and cell viability assay*

For drug treatments of protoplasts, the following substances were added from stock solutions for the indicated times to 500 µl of protoplast suspension: 1 mM $LaCl_3$ (5 min), 2 mM $H_2O_2$ (5 min), 3 mM NEM (20 min), 5 mM DTT (30 min). Protoplasts were incubated at room temperature with gentle stirring (5 rpm). 15 min after treatments, protoplast viability was determined with the FDA test (39). For drug treatments of plants, one leaf per plant was sprayed with 10 mM $LaCl_3$, 20 mM $H_2O_2$ or with water, and the leaf, still attached to the plant, used for transmission experiments after the applied solutions had evaporated.

*Aphid transmission tests*

A nonviruliferous clonal *Myzus persicae* colony was reared under controlled conditions (22/18 °C day/night with a photoperiod of 14/10 h day/night) on eggplant. The transmission tests using protoplasts were performed as described (6), with an acquisition access period of 15 min and transferring 10 aphids to each test plant. For plant-to-plant transmission tests, an acquisition time of 2 min was used and only one aphid was transferred on each turnip plant for inoculation. Infected plants were identified by visual inspection for symptoms 3 weeks after inoculation.

*Antisera*

The following primary antibodies were used: commercial rabbit anti-TuMV (sediag.com) and mouse and rabbit anti-HC-Pro (recognizing HC-Pro from different potyviruses, produced against the conserved peptide SEIKMPTKHHLVIGNSGDPKYIDLP by proteogenix.fr and eurogentec.com, respectively). The following secondary antibodies were used: Alexa Fluor 488 and 594 anti-rabbit and anti-mouse conjugates (thermofisher.com) for immunofluorescence, anti-rabbit IgG conjugated to alkaline phosphatase (www.sigmaaldrich.com) for western blotting and corresponding Minus and Plus probes (www.sigmaaldrich.com) for Duolink®.

*Immunofluorescence*

Protoplasts were fixed with 1 % glutaraldehyde and processed as described (6). The primary and secondary antibodies were used at 1:100 and 1:200 dilutions, respectively.

*Western blotting*

Drug treatments of protoplasts were stopped by lysing protoplasts in non-reducing 2x Laemmli buffer (v/v) (40) except where indicated otherwise. Optionally, oligomer formation was stabilized by incubating protoplasts with 3 mM NEM for 20 min before lysis. This step yielded sharper oligomer bands. Samples were then resolved by 10 % SDS-PAGE. Proteins were transferred to nitrocellulose membranes and incubated with primary and secondary antibodies as described (6) except that TuMV-specific primary antibodies (1:1000 dilution) were used. Antigens were then revealed by the NBT/BCIP reaction. Equal protein charge on the membranes was verified by coloring the RuBisCO with Ponceau S Red.

*Duolink® proximity ligation assay*

*In situ* protein/protein interactions were detected by proximity ligation assay using the Duolink® kit (www.sigmaaldrich.com). Protoplasts were isolated from healthy or infected (14 dpi) turnip leaves and fixed with 3 % paraformaldehyde in 100 mM cacodylate buffer (pH 7.2) or 100 mM phosphate buffer (pH 7.4). The fixed protoplasts were immobilized on L-polylysine-coated slides. Antibody incubation with rabbit anti-TuMV and mouse anti-HC-Pro, ligation and probe amplification were performed according to the manufacturer's instructions. The slides were mounted with Duolink® *in situ* mounting medium with DAPI (www.sigmaaldrich.com).

*Microscopy*

Immunolabeled protoplasts were observed with an Olympus BX60 epifluorescence microscope (olympus-lifescience.com) equipped with GFP and Texas Red narrow band filters and images acquired with a color camera. Duolink® images were acquired with a Zeiss LSM700 confocal microscope (zeiss.com) operated in sequential mode. DAPI was exited with the 405 nm laser and fluorescence collected from 405-500 nm, Duolink® probes and chlorophyll were excited with the 488 nm laser and fluorescence collected from 490-540 nm (Duolink® signal)or from 560-735 nm (chlorophyll autofluorescence). Raw images were processed using ZEN or ImageJ software. Quantification of Duolink® interactions was performed on maximum intensity projections with the Analyse_Spots_Per_Protoplast macro for ImageJ, developed for this experiment (41).

*Statistical analysis*

Statistics and box plots were calculated with R software version 3.4.0 (r-project.org). Transmission rates and cell viability were analyzed with generalized linear models (GLM). Quasi-binomial distributions were used in order to take overdispersion into account, and p-values were corrected with the Holm method (42) to account for multiple comparisons.

Analyzing the Duolink® experiments required the calculation of the total fluorescence intensity ($F_{tot}$) of labeled foci as:

$$F_{tot} = \frac{n \times \bar{s} \times \bar{I}}{A}$$

where $n$ is the number of labeled foci, $\bar{s}$ the average size of a focus, $\bar{I}$ the average fluorescence intensity of a focus and $A$ the size of the protoplast. $F_{tot}$ was log-transformed (to normalize the distribution) and analyzed with linear models using "treatment" and "replicate" as categorical explanatory variables.

**References**


1. Blanc S, Drucker M, Uzest M. 2014. Localizing viruses in their insect vectors. Annu Rev Phytopathol 52:403–425.

2. Dáder B, Then C, Berthelot E, Ducousso M, Ng JCK, Drucker M. 2017. Insect transmission of plant viruses: Multilayered interactions optimize viral propagation. Insect Sci 24:929–946.

3. Kuno G, Chang G-JJ. 2005. Biological transmission of arboviruses: reexamination of and new insights into components, mechanisms, and unique traits as well as their evolutionary trends. Clin Microbiol Rev 18:608–637.

4. Lefèvre T, Adamo SA, Biron DG, Missé D, Hughes D, Thomas F. 2009. Invasion of the body snatchers: the diversity and evolution of manipulative strategies in host-parasite interactions. Adv Parasitol 68:45–83.

5. Matthews KR. 2011. Controlling and coordinating development in vector-transmitted parasites. Science 331:1149–1153.

6. Martinière A, Bak A, Macia J-L, Lautredou N, Gargani D, Doumayrou J, Garzo E, Moreno A, Fereres A, Blanc S, Drucker M. 2013. A virus responds instantly to the presence of the vector on the host and forms transmission morphs. eLife 2:e00183.

7. Drucker M, Then C. 2015. Transmission activation in non-circulative virus transmission: a general concept? Curr Opin Virol 15:63–68.

8. Drucker M, Froissart R, Hébrard E, Uzest M, Ravallec M, Espérandieu P, Mani J-C, Pugnière M, Roquet F, Fereres A, Blanc S. 2002. Intracellular distribution of viral gene products regulates a complex mechanism of cauliflower mosaic virus acquisition by its aphid vector. Proc Natl Acad Sci USA 99:2422–2427.

9. Espinoza AM, Medina V, Hull R, Markham PG. 1991. Cauliflower mosaic virus gene II product forms distinct inclusion bodies in infected plant cells. Virology 185:337–344.

10. Bak A, Gargani D, Macia J-L, Malouvet E, Vernerey M-S, Blanc S, Drucker M. 2013. Virus factories of Cauliflower mosaic virus are virion reservoirs that engage actively in vector-transmission. J Virol.

11. Martinière A, Macia J-L, Bagnolini G, Jridi C, Bak A, Blanc S, Drucker M. 2011. VAPA, an Innovative "Virus-Acquisition Phenotyping Assay" Opens New Horizons in Research into the Vector-Transmission of Plant Viruses. PLoS One 6.

12. Peng H-C, Walker GP. 2018. Sieve element occlusion provides resistance against Aphis gossypii in TGR-1551 melons. Insect Sci.

13. Baunoch DA, Das P, Hari V. 1990. Potato virus Y helper component protein is associated with amorphous inclusions. J Gen Virol 71 ( Pt 10):2479–2482.

14. Riedel D, Lesemann DE, Maiss E. 1998. Ultrastructural localization of nonstructural and coat proteins of 19 potyviruses using antisera to bacterially expressed proteins of plum pox potyvirus. Arch Virol 143:2133–2158.

15. Söderberg O, Gullberg M, Jarvius M, Ridderstråle K, Leuchowius K-J, Jarvius J, Wester K, Hydbring P, Bahram F, Larsson L-G, Landegren U. 2006. Direct observation of individual endogenous protein complexes in situ by proximity ligation. Nat Methods 3:995–1000.

16. Plisson C, Drucker M, Blanc S, German-Retana S, Le Gall O, Thomas D, Bron P. 2003. Structural characterization of HC-Pro, a plant virus multifunctional protein. J Biol Chem 278:23753–23761.

17. Ruiz-Ferrer V, Boskovic J, Alfonso C, Rivas G, Llorca O, López-Abella D, López-Moya JJ. 2005. Structural analysis of tobacco etch potyvirus HC-pro oligomers involved in aphid transmission. J Virol 79:3758–3765.

18. Thornbury DW, Hellmann GM, Rhoads RE, Pirone TP. 1985. Purification and characterization of potyvirus helper component. Virology 144:260–267.

19. Modis Y, Trus BL, Harrison SC. 2002. Atomic model of the papillomavirus capsid. EMBO J 21:4754–4762.

20. Zebelo SA, Maffei ME. 2015. Role of early signalling events in plant-insect interactions. J Exp Bot 66:435–448.

21. Vincent TR, Avramova M, Canham J, Higgins P, Bilkey N, Mugford ST, Pitino M, Toyota M, Gilroy S, Miller AJ, Hogenhout SA, Sanders D. 2017. Interplay of Plasma Membrane and Vacuolar Ion Channels, Together with BAK1, Elicits Rapid Cytosolic Calcium Elevations in Arabidopsis during Aphid Feeding. Plant Cell 29:1460–1479.

22. Jeworutzki E, Roelfsema MRG, Anschütz U, Krol E, Elzenga JTM, Felix G, Boller T, Hedrich R, Becker D. 2010. Early signaling through the Arabidopsis pattern recognition receptors FLS2 and EFR involves Ca-associated opening of plasma membrane anion channels. Plant J 62:367–378.

23. Lachaud C, Da Silva D, Amelot N, Béziat C, Brière C, Cotelle V, Graziana A, Grat S, Mazars C, Thuleau P. 2011. Dihydrosphingosine-induced programmed cell death in tobacco BY-2 cells is independent of $H_2O_2$ production. Mol Plant 4:310–318.

24. Miles PW. 1999. Aphid Saliva. Biological Reviews 74:41–85.

25. Jones JDG, Dangl JL. 2006. The plant immune system. Nature 444:323–329.

26. Hyodo K, Hashimoto K, Kuchitsu K, Suzuki N, Okuno T. 2017. Harnessing host ROS-generating machinery for the robust genome replication of a plant RNA virus. Proc Natl Acad Sci USA 114:E1282–E1290.

27. Fan SW, George RA, Haworth NL, Feng LL, Liu JY, Wouters MA. 2009. Conformational changes in redox pairs of protein structures. Protein Sci 18:1745–1765.

28. Mou Z, Fan W, Dong X. 2003. Inducers of plant systemic acquired resistance regulate NPR1 function through redox changes. Cell 113:935–944.

29. Zaffagnini M, Fermani S, Costa A, Lemaire SD, Trost P. 2013. Plant cytoplasmic GAPDH: redox post-translational modifications and moonlighting properties. Front Plant Sci 4:450.

30. Govier DA, Kassanis B. 1974. A virus induced component of plant sap needed when aphids acquire potato virus Y from purified preparations. Virology 61:420–426.

31. Atreya CD, Atreya PL, Thornbury DW, Pirone TP. 1992. Site-directed mutations in the potyvirus HC-Pro gene affect helper component activity, virus accumulation, and symptom expression in infected tobacco plants. Virology 191:106–111.

32. Cronin S, Verchot J, Haldeman-Cahill R, Schaad MC, Carrington JC. 1995. Long-distance movement factor: a transport function of the potyvirus helper component proteinase. Plant Cell 7:549–559.

33. Anandalakshmi R, Marathe R, Ge X, Herr JM, Mau C, Mallory A, Pruss G, Bowman L, Vance VB. 2000. A calmodulin-related protein that suppresses posttranscriptional gene silencing in plants. Science 290:142–4.

34. Brigneti G, Voinnet O, Li WX, Ji LH, Ding SW, Baulcombe DC. 1998. Viral pathogenicity determinants are suppressors of transgene silencing in Nicotiana benthamiana. EMBO J 17:6739–6746.

35. Kasschau KD, Carrington JC. 1998. A counterdefensive strategy of plant viruses: suppression of posttranscriptional gene silencing. Cell 95:461–70.

36. Ohshima K, Tomitaka Y, Wood JT, Minematsu Y, Kajiyama H, Tomimura K, Gibbs AJ. 2007. Patterns of recombination in turnip mosaic virus genomic sequences indicate hotspots of recombination. J Gen Virol 88:298–315.

37. Revers F, Yang SJ, Walter J, Souche S, Lot H, Le Gall O, Candresse T, Dunez J. 1997. Comparison of the complete nucleotide sequences of two isolates of lettuce mosaic virus differing in their biological properties. Virus Res 47:167–177.

38. Sako N, Ogata K. 1981. Different helper factors associated with aphid transmission of some potyviruses. Virology 112:762–765.

39. Widholm JM. 1972. The use of fluorescein diacetate and phenosafranine for determining viability of cultured plant cells. Stain Technol 47:189–194.

40. Laemmli UK. 1970. Cleavage of Structural Proteins during the Assembly of the Head of Bacteriophage T4. Nature 227:680–685.

41. Baecker V. 2016. Analyse Spots Per Protoplast - ImageJ-macros - MRI's Redmine.

42. Holm S. 1979. A simple sequentially rejective multiple test procedure. Scand J Statist 6:65–70.

43. Bak A, Martinière A, Blanc S, Drucker M. 2013. Early interactions during the encounter of plants, aphids and arboviruses. Plant Signal Behav 8:e24225.

**Acknowledgments**

We are grateful to Takii Europe for providing turnip seeds. Our work is financed by INRA SPE department, Agence Nationale de la Recherche (ANR) grant 12-BSV7-005-01, awarded to MD, and grant RGP0013/2015 from Human Frontier Science Program (HFSP), awarded to MD. EB is supported by CIFRE PhD fellowship N° 2015/1115, financed by Association Nationale Recherche Technologie (anrt), Semences Innovation Protection Recherche et Environnement (SIPRE) and Fédération Nationale des Producteurs de Plants de Pomme de Terre (FN3PT). We thank Albin Teulet for help with the box plots and Sophie Le Blaye for plant care. All authors declare that there is no conflict of interest.

## Legends to Figures

**Figure 1**. Effect of $H_2O_2$ and $LaCl_3$ on TuMV transmission by aphids. (A-B) Turnip protoplasts were incubated for 5 min with 2 mM $H_2O_2$ (A) or 1 mM $LaCl_3$ (B) and then employed in transmission assays. (C-D) Cell viability of protplasts was measured to determine if the altered transmission rates were due to modified viability. (E-F) Cell extracts from protoplasts were treated identically with $H_2O_2$ (C) or $LaCl_3$ (D) and used in transmission assays. (G-H) Leaves on intact plants were sprayed with 20 mM $H_2O_2$ (E) or 10 mM $LaCl_3$ (F) and then employed in transmission assays. Means of infected test plants (horizontal black bars in the box plots) are calculated from a pool of three independent experiments in which a total of 360 tests plants were used per condition. Each experiment had 6 repetitions for each condition and 20 tests plants per repetition (see Supplementary Data Set S1 for raw data). *p* designates p-values obtained by generalized linear models (see materials and methods). The box plots here and in the other figures present medians, upper and lower quartiles, the ends of the whiskers present lowest and highest datum still within 1.5 IQR of the lower and higher quartile, respectively, and the circles show outliers.

**Figure 2.** Immunofluorescence of turnip protoplasts infected with TuMV. TuMV-infected protoplasts were treated as indicated and double-labeled against HC-Pro (green, first column) and viral capsid protein CP (red, middle column). The right column (Merge) represents superposition of HC-Pro and CP labels, with co-labeling appearing in yellow. Control, untreated protoplasts; $H_2O_2$, incubation with 2 mM $H_2O_2$ for 15 min, $LaCl_3$, incubation with 1 mM $LaCl_3$ for 15 min. Scale bars 50 µm.

**Figure 3.** *In situ* Duolink® proximity ligation assay on turnip protoplasts infected with TuMV. (A) Untreated control protoplasts or protoplasts incubated with either $H_2O_2$ or $LaCl_3$ were processed by Duolink® for detection of HC-Pro/TuMV particle interactions using HC-Pro and CP antibodies and corresponding Duolink® probes. Interactions are visible as green fluorescing spots. Nuclei were counterstained with DAPI (blue) and chloroplast autofluorescence is presented in grey to reveal the cell lumen. Scale bars: 20 µm. (B-C) Quantitative analysis of the Duolink® signal shows that (B) $H_2O_2$ increased and (C) $LaCl_3$ decreased HC-Pro/CP interactions. The box plots presents data from three independent experiments using between 56-115 protoplasts for each condition. The y-axes show HC-Pro/CP interactions, presented as total fluorescent intensity ($F_{tot}$). *p* designates p -values obtained by generalized linear models (see material and methods).

**Figure 4.** Non-reducing SDS-PAGE/Western blotting analysis of HC-Pro and CP from TuMV-infected turnip protoplasts. The samples were lysed in a buffer without reducing agents to conserve the disulfide bridges. (A) $H_2O_2$ and $LaCl_3$ treatments did not modify the migration profile of the capsid protein (CP), whereas they (B) induced ($H_2O_2$) or inhibited ($LaCl_3$) formation of HC-Pro oligomers. (C-D) The concentration range and the kinetics of $H_2O_2$ incubation shows that HC-Pro oligomerization (C) was induced by a minimum concentration of 0.25 mM and (D) that it was rapid and reversible, either by extended $H_2O_2$ treatment (left panel) or by washing protoplasts (right panel). (E) Also inhibition of HC-Pro oligomerization by $LaCl_3$ was rapid and reversible. (F-G) HC-Pro oligomers are formed by intermolecular disulfide bridges because (F) incubation of protoplasts with DTT, either alone or after $H_2O_2$ treatment, abolished HC-Pro oligomers, and (G) treatment with NEM before but not after previous incubation with $H_2O_2$ prevented their formation. (H) Transmission tests using NEM-treated protoplasts show a drastic diminution of TuMV transmission. Transmission tests were performed three times using 320 plants per condition and analyzed by generalized linear models as described in Figure 1. (I) Protoplast viability assays show that NEM treatment did not change cell viability under the conditions used. TuMV, samples of TuMV-infected protoplasts; Non inf., samples of non infected protoplasts; $LaCl_3$, treatment with 1 mM $LaCl_3$ for 5 min; $H_2O_2$, treatment with 2 mM $H_2O_2$ for 5 min; wash, $H_2O_2$ was removed by centrifugation and resuspension of protoplasts in fresh medium; DTT, treatment with 5 mM DTT for 30 min; NEM, treatment with 3 mM NEM for 20 min. Equal loading of lanes is shown by Ponceau Red staining of the large RuBisCO subunit (Rub). A precolored ladder and the molecular masses in kDa are indicated at one side of each blot. $p$ in (H) designates p-value obtained by generalized linear models from three independent experiments.

**Figure 5.** Model of TuMV acquisition by aphids. For simplicity, aphids, viral components and the plant cell are not drawn to scale. (1) Before the arrival of aphid vectors, the redox potential of the cytosol of TuMV-infected cells has 'normal' values, i.e. it is reduced. Consequently, the cytosolic HC-Pro protein (blue circles) is in a reduced form (the red points in HC-Pro present reduced cysteines) and contains no intermolecular disulfide bridges. This form of HC-Pro is presumably not associated with virus particles (purple lines). It is likely but remains to be confirmed whether reduced HC-Pro is dimeric as presented here. (2) When an aphid feeds on a leaf infected with TuMV, an unknown elicitor is recognized by the plant cell and induces the opening of calcium channels (pink cylinder) and triggers directly or indirectly ROS production in the cell. During this activation stage, the ROS in the cytoplasm increases (red lightning) the redox potential of the cell cytoplasm and oxidizes one or more HC-Pro cysteines. This oxidation

generates disulfide bridges (red lines) between different HC-Pro molecules. The intermolecular disulfide bridges either induce oligomerization of a portion of HC-Pro or change the conformation of a part of existing oligomers, presented by the transition of the circles to squares. For simplicity, higher HC-Pro forms are not shown. (3) Whatever the case, oxidation of a fraction of HC-Pro results in a functional switch of the protein and the oxidized tertiary or quaternary conformation allows interaction between HC-Pro and TuMV particles and the formation of TuMV transmissible complexes, symbolized by square HC-Pro aligned with a virion. Now the infected cell is switched into transmission mode and this stage allows efficient acquisition of TuMV. (4) The aphid acquires transmissible complexes and transmits the TuMV during the next punctures on another plant. After vector departure, the redox potential of cell cytoplasm lowers again and HC-Pro is reduced. This changes its conformation and induces dissociation of the transmissible complexes, leaving HC-Pro free to fulfill its other functions during infection. The aphid drawing is modified from (43), published under open CC3.0 license.

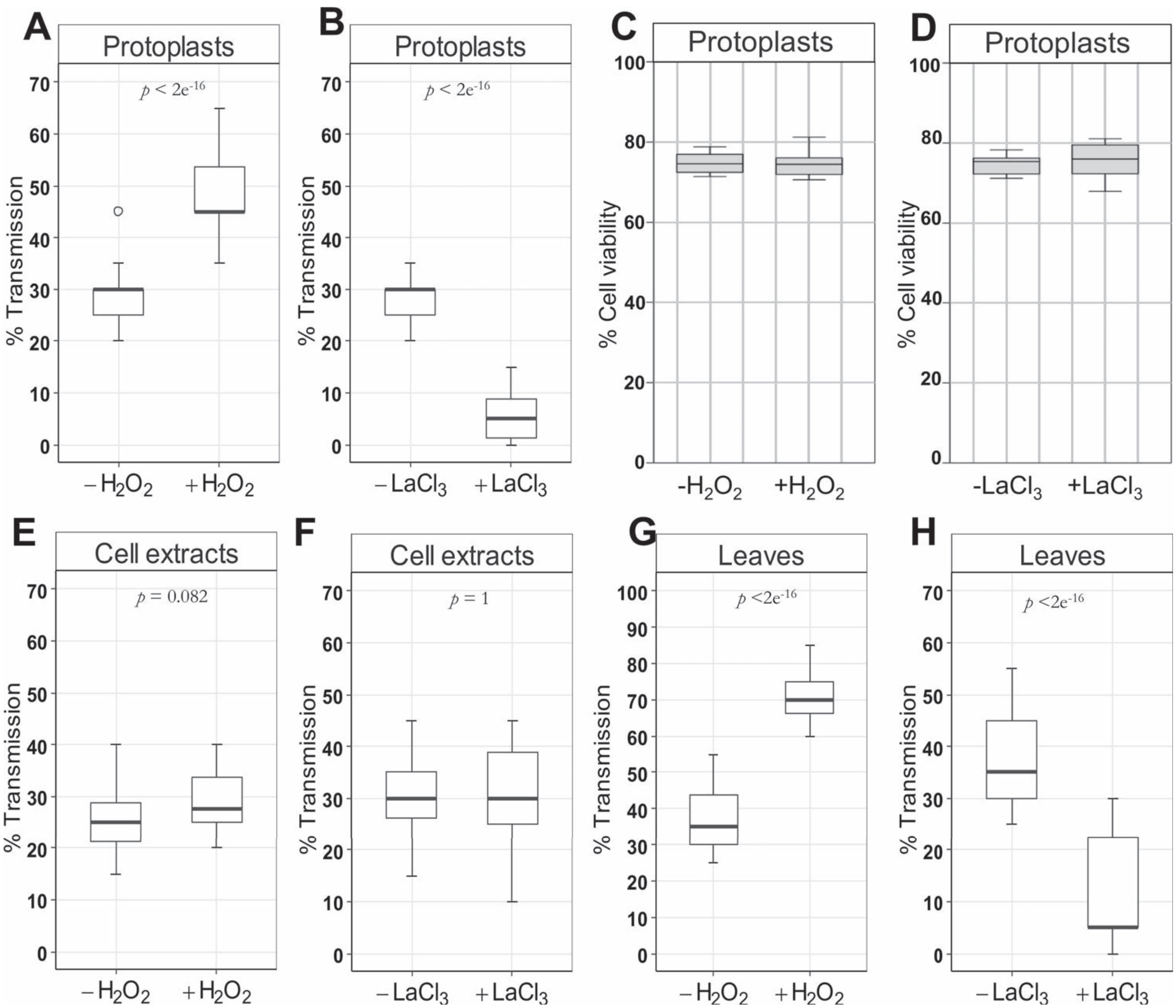
A
Protoplasts
$p < 2e^{-16}$
% Transmission
$-H_2O_2$
$+H_2O_2$
B
Protoplasts
$p < 2e^{-16}$
% Transmission
$-LaCl_3$
$+LaCl_3$
C
Protoplasts
% Cell viability
$-H_2O_2$
$+H_2O_2$
D
Protoplasts
% Cell viability
$-LaCl_3$
$+LaCl_3$
E
Cell extracts
$p = 0.082$
% Transmission
$-H_2O_2$
$+H_2O_2$
F
Cell extracts
$p = 1$
% Transmission
$-LaCl_3$
$+LaCl_3$
G
Leaves
$p < 2e^{-16}$
% Transmission
$-H_2O_2$
$+H_2O_2$
H
Leaves
$p < 2e^{-16}$
% Transmission
$-LaCl_3$
$+LaCl_3$

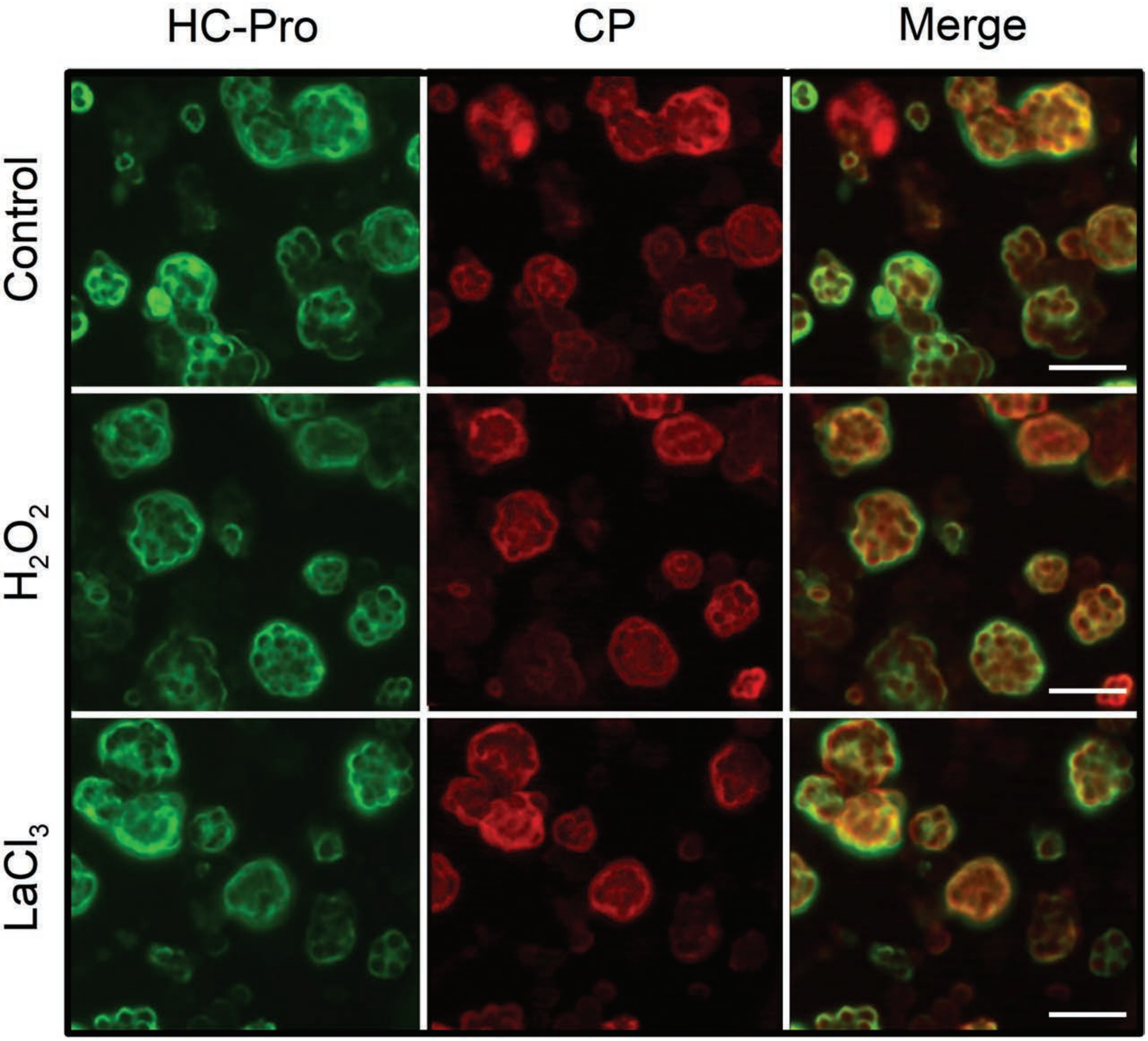
HC-Pro
CP
Merge
Control
$H_2O_2$
$LaCl_3$

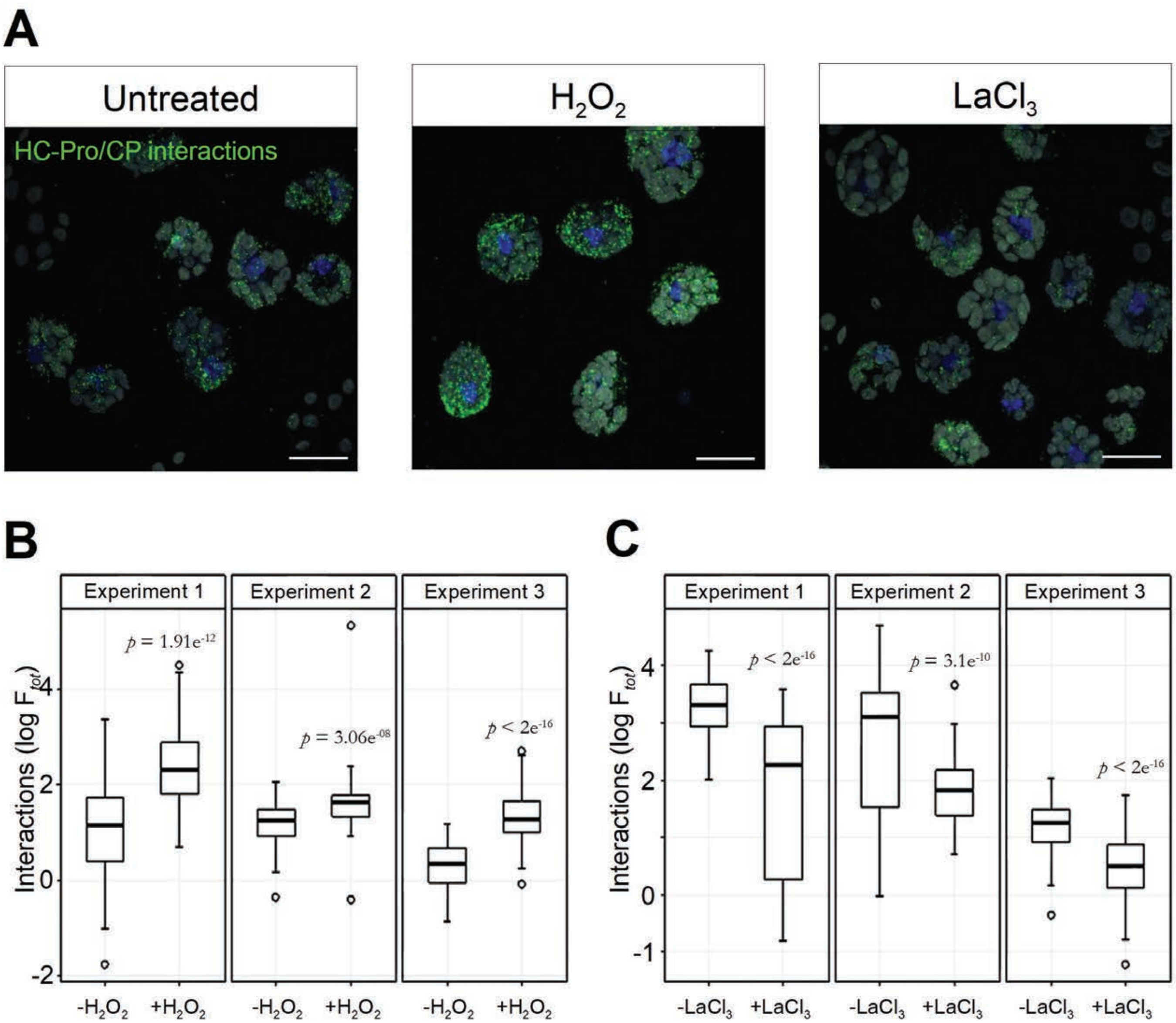
A
Untreated
H2O2
LaCl3
HC-Pro/CP interactions
B
C
Experiment 1
Experiment 2
Experiment 3
Interactions (log Ftot)
p = 1.91e-12
p = 3.06e-08
p < 2e-16
p < 2e-16
p = 3.1e-10
p < 2e-16
-H2O2
+H2O2
-LaCl3
+LaCl3

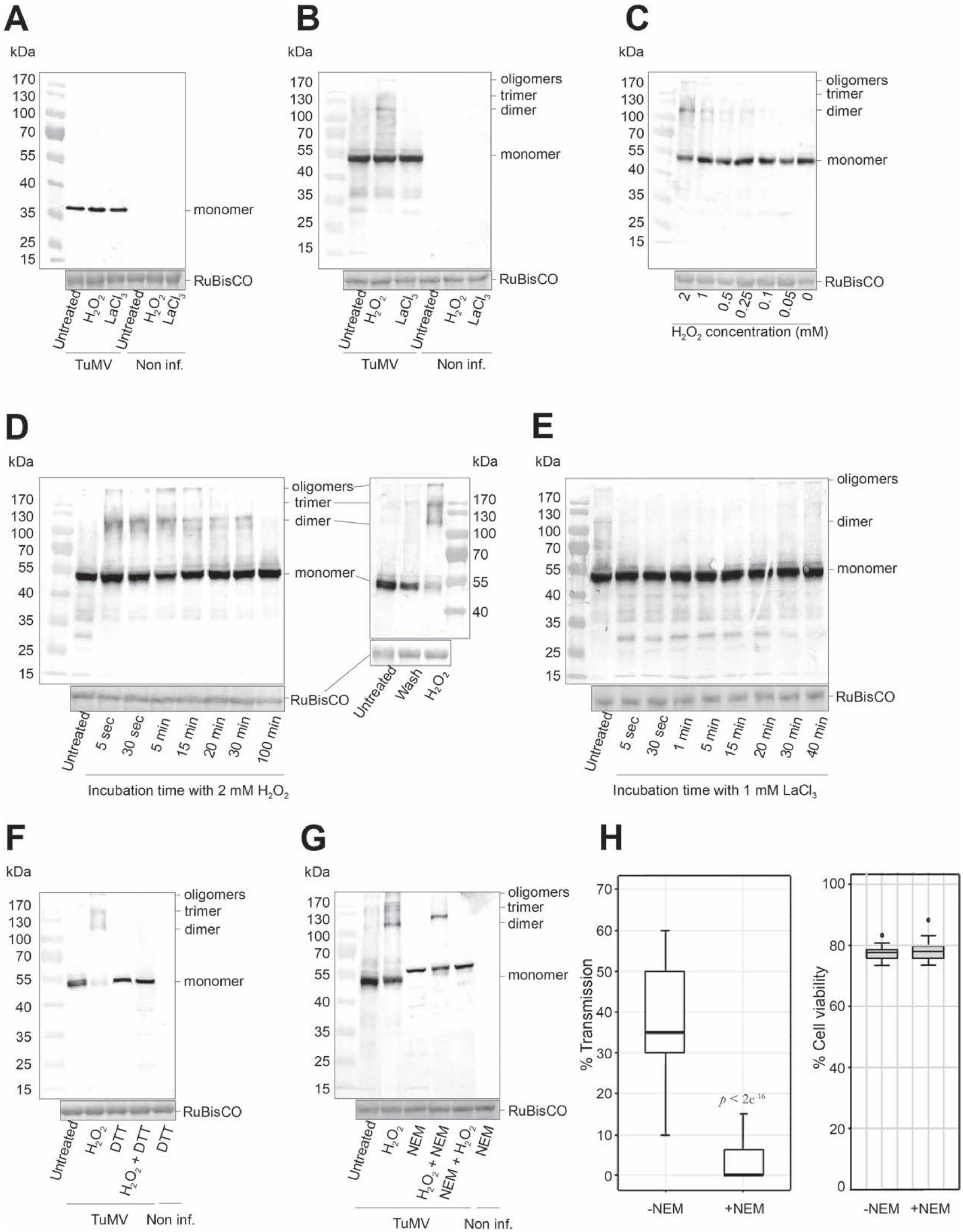
A
kDa
170
130
100
70
55
40
35
25
15
monomer
RuBisCO
Untreated
$H_2O_2$
$LaCl_3$
Untreated
$H_2O_2$
$LaCl_3$
TuMV
Non inf.
B
kDa
oligomers
trimer
dimer
monomer
RuBisCO
Untreated
$H_2O_2$
$LaCl_3$
Untreated
$H_2O_2$
$LaCl_3$
TuMV
Non inf.
C
kDa
oligomers
trimer
dimer
monomer
RuBisCO
2
1
0.5
0.25
0.1
0.05
0
$H_2O_2$ concentration (mM)
D
kDa
oligomers
trimer
dimer
monomer
RuBisCO
Untreated
5 sec
30 sec
5 min
15 min
20 min
30 min
100 min
Incubation time with 2 mM $H_2O_2$
Untreated
Wash
$H_2O_2$
E
kDa
oligomers
dimer
monomer
RuBisCO
Untreated
5 sec
30 sec
1 min
5 min
15 min
20 min
30 min
40 min
Incubation time with 1 mM $LaCl_3$
F
kDa
oligomers
trimer
dimer
monomer
RuBisCO
Untreated
$H_2O_2$
DTT
$H_2O_2$ + DTT
DTT
TuMV
Non inf.
G
kDa
oligomers
trimer
dimer
monomer
RuBisCO
Untreated
$H_2O_2$
NEM
$H_2O_2$ + NEM
NEM + $H_2O_2$
NEM
TuMV
Non inf.
H
% Transmission
$p < 2e^{-16}$
-NEM
+NEM
% Cell viability
-NEM
+NEM

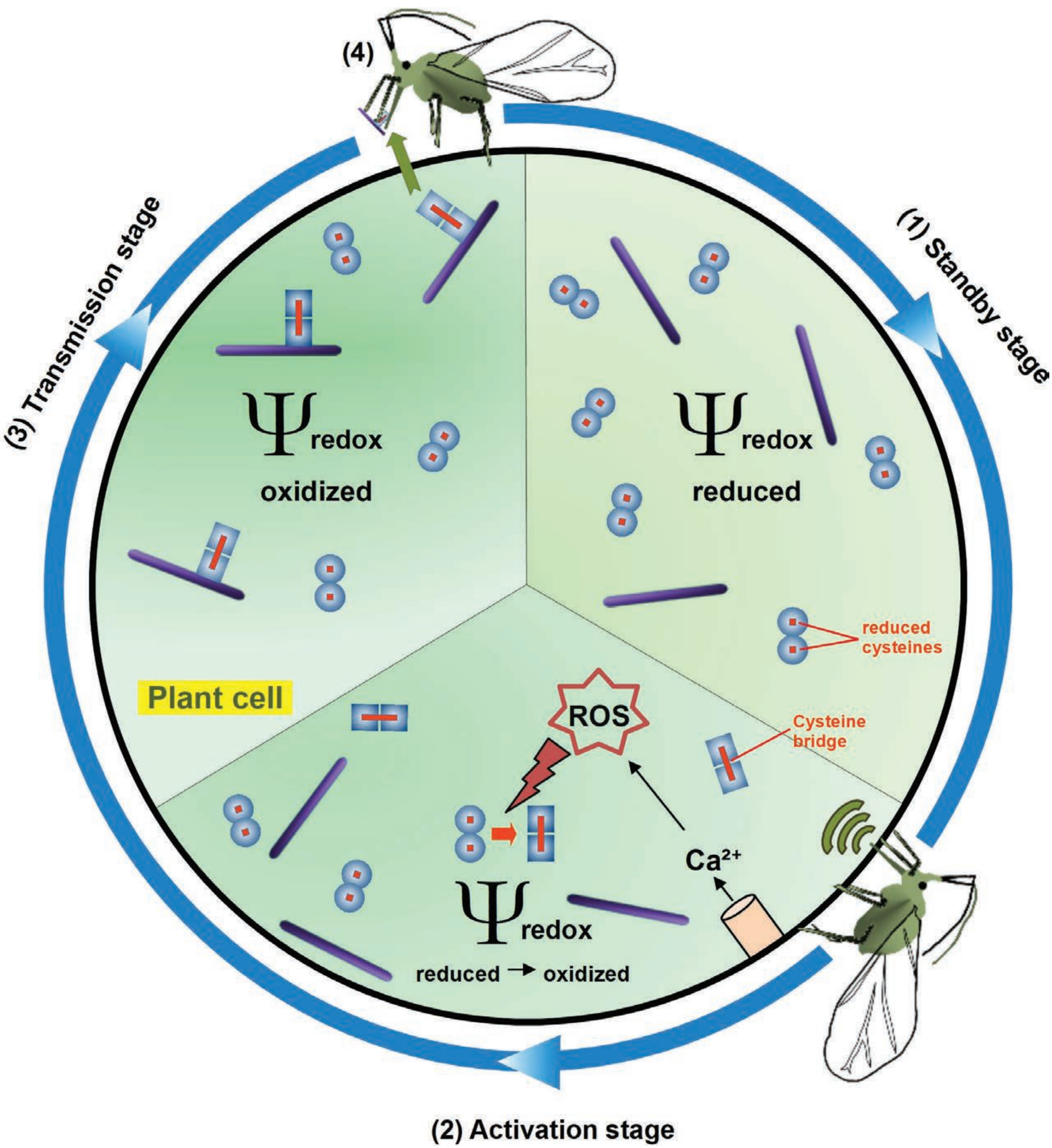
(4)
(1) Standby stage
(2) Activation stage
(3) Transmission stage
Ψredox
reduced
Ψredox
oxidized
Ψredox
reduced → oxidized
reduced
cysteines
Cysteine
bridge
ROS
Ca²⁺
Plant cell